GROWTH AND ETCHING OF HEXAGONAL BORON NITRIDE

———CONTROL OF NUCLEATION AND CRYSTAL MORPHOLOGY

A Thesis

Presented to the Faculty of the Graduate School

of Cornell University

In Partial Fulfillment of the Requirements for the Degree of

Master of Science Professional Studies

by

Yanxin Ji

August 2016

ABSTRACT

Hexagonal boron nitride (h-BN) is a layered material and it is similar to graphene in lattice structure. Sheets of h-BN are composed of alternating boron and nitrogen atoms in a honeycomb arrangement. The strong bond between boron and nitrogen leads to the formation of a wide bandgap (5.9eV) material. The layers are held together by weak van der Waals forces as other layered materials. Since their superb chemical stability and intrinsic insulation, h-BN can be used as a thin top dielectric layer to gate graphene and as an inert substrate for graphene transistors. So the strategy to grow high quality h-BN on a large scale is very important. My research focuses on the controllable growth of h-BN on copper substrates using the low-pressure chemical vapor deposition (LPCVD) method. In order to optimize the growth condition, I investigated how the precursor, geometric environment, substrate engineering and gas mixture affect the quality of the as-grown h-BN. Electropolishing of the Cu substrate was used to reduce the nucleation density of h-BN and hence the domain sizes increase. The evolution of varied h-BN domain shapes was explained by the underlying growth mechanism. Raman, SEM, XPS, and LEEM I-V Curve were performed on the samples for characterization. In the last part, I will show the electric properties of the device made by the as-grown h-BN.

BIOGRAPHICAL SKETCH

Yanxin Ji was born and raised up in Pinghu, China. From childhood, he is a curious person of wide interest. His skills in calligraphy, swimming and track and field were formed by years of practice and left him a qualified participant in campus and social activities.

In his third year of high school, he won a gold medal at the National Physics Olympic and earned admission to Peking University. He chose Physics as his major. His interest in material science was sparked from the course of History of Science in high school. Once his teacher told him that the discovery of new materials always triggered a profound revolution in science, he was deeply attracted by that idea. Therefore, He chose physics as his undergraduate major since he realized that a solid base in physics is required to research new materials.

Chinese materials technology is relatively backward, while the U.S. has a leading position in the field of material science. Therefore he went to U.S, for his graduate study in Materials Science. He hopes the experience of a Master program can significantly enrich his knowledge, enhance his expertise, sharpen his research skills and then allow him to use his advanced knowledge to advance material enterprises in China.

Dedicated to all the folks that helped get me here, but especially to my parents: for always supporting me and encouraging me.

ACKNOWLEDGMENTS

First of all, I would like to express my sincere gratitude to my parents, Fuming Ji and Lingjuan Dai, for letting me know what kind of man I should be.

To Professor Michael Spencer, thank you for accepting me into your group and your continues guidance and advise. Thank you for letting me work for the materials growth project, which I'm very interested in. I have learned so much from you and I am eternally grateful.

To my committee members, Professor Debdeep Jena, thank you for agreeing to be on my committee, despite your busy schedules. Your class is so great and I learnt a lot from it.

I would also like to acknowledge my group mates and my collaborators to the work presented here in this dissertation. I would like to thank Brian Calderon, who was always willing to help answer questions and help with experimental set ups. To Jeonghyun Hwang, thank you for helping me to get into the research world and your always awesome ideas. To Hussain Alsalman and Joon Young Kwak, I'm so gad to be in the same group with you and thank you for the helpful discussions. I also want to thank Johannes Jobst for the LEEM measurement.

To my room mates Mian Pan, Lingyuan Zhu and Yuhui Zhou, I had a really wonderful time with you in the past two years.

To my fellow master students outside of my research group, there are too many awesome people to list, but thank you all for the memories (parties, paintball and skiing come to mind) and good times

TABLE OF CONTENTS

LIST OF FIGURES

CHAPTER 1

INTRODUCTION

1.1 Hexagonal Boron Nitride

In recent years, graphene has received continuous attention for its intriguing optical and electronic properties. Since then, single and few-atom-thick layers of van der Waals materials, has been widely researched. Hexagonal boron nitride (h-BN) is among the most studied layered material after graphene. Similar to graphene, h-BN has a wide range of application. So the strategy to grow high quality h-BN on a large scale is very important.

Hexagonal boron nitride (h-BN) is a layered material and it is similar to graphene in lattice structure [1]. Sheets of h-BN are composed of alternating boron and nitrogen atoms in a honeycomb arrangement. The strong bond between boron and nitrogen leads to the formation of a wide bandgap (5.9eV) material [2]. The layers are held together by weak van der Waals forces as other layered materials [1]. Since their superb chemical stability and intrinsic insulation, h-BN can be used as a thin top dielectric layer to gate graphene and as an inert substrate for graphene transistors [3].

1.2 Chemical Vapor Deposition

Chemical vapor deposition (CVD) is a kind of thin film growth method that plays an important role in the growth of low-dimension materials. It provides an ability to accurately control the chemical composition and structure in a relatively low temperature. In essence, CVD is a material synthesis process used to produce high quality solid materials. When the synthesis proceeds, vapor atoms/ molecules are transported to the vicinity of the substrate surface and then react at the substrate surface to produce thin films [4].

Thin films can be prepared using a variety of technologies according to different requirements. Compared to other growth methods, CVD has these unique advantages: 1) The ability to control film stoichiometry over a wide range. 2) The ability to produce large scale films. 3) Affordability of equipment and operating expenses. 4) Suitability for both batch and semicontinuous operation. 5) Compatibility with other processing steps [4].

Similar to MoS2, although several methods for synthesis h-BN such as exfoliation or wet chemical reactions have been reported, these methods cannot control the quality of film structure and the number of layers well. So the CVD method has been explored in order to have fine control over the layer number and lateral size [5].

1.3 Growth Method and System Introduction

Figure 1.1 shows the schematic illustration of our CVD system for synthesis of monolayer h-BN. The system is composed by a quartz tube and a hot wall furnace. The sample was wrapped on to a quartz boat. The boat can be moved between a hot zone (center of the furnace) and a cold zone (outside the furnace). A bubbler is made ahead of the tube separated by a valve. The bubbler is used to place the precursor. A small inlet is made at the side of the tube for flowing the reaction and carrier gases.

Copper foils were used as the substrate. They were first treated with electro-polishing. The copper was wrapped on to a quartz boat. And then the boat was loaded into the quartz tube. The chamber was pumped down to a base pressure of ~10–3 torr using a turbo pump and the furnace temperature was heated to 1050 °C under vacuum. When the hot zone temperature was stable, the copper was pre-cleaned in the cold zone for

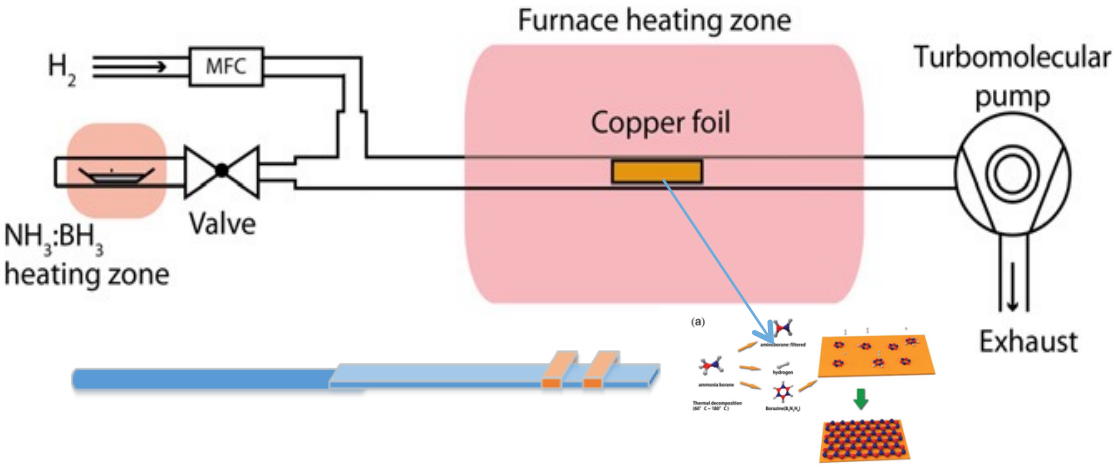

Figure 1.1: Schematic illustration of a typical CVD system for synthesis

30min under 40 standard cubic centimeters (sccm) of hydrogen. After that, the foil was transferred into the hot zone and was annealed for 60 min at 1050 °C prior to growth (Figure 1.2).

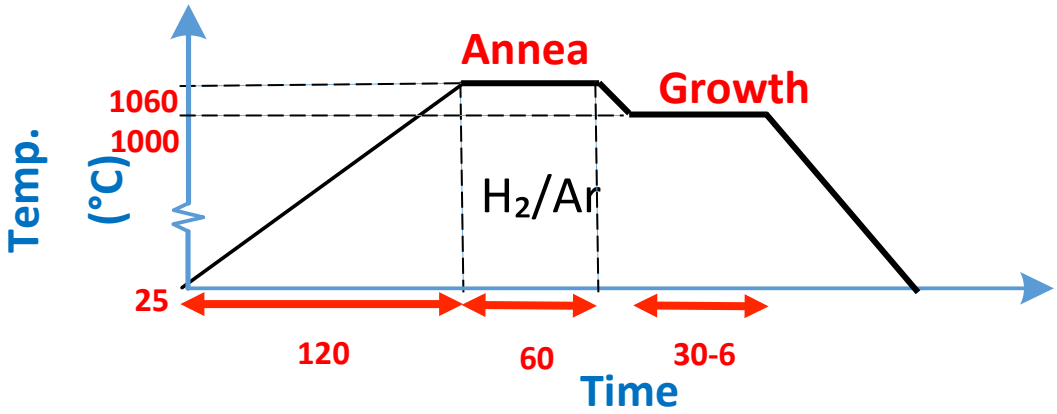

Figure 1.2: Illustration of growth procedure

Ammonia borane was used as the precursor. 100 mg of ammonia borane was placed in a bubbler ahead of the tube, separated from the furnace by a valve. The precursor was heated by heating tapes. After a period of time of anneal, the bubbler temperature was increased to 70℃ and the furnace temperature was decrease to 1000℃.

Growth was initiated by opening the valve to the ammonia borane. 10 sccm hydrogen was flowed during growth. After a period of time of growth, the valve to the precursor was closed and the copper foil was removed out of the hot zone immediately. The furnace was opened to cool down. The post-growth environment was under 10 sccm hydrogen combined with 20 sccm Argon.

1.4 Precursor Chemistry

Ammonia borane was used as the precursor for its volatility at low temperature. It is solid at room temperature with B and N atoms in 1:1 stoichiometric ratio [6]. Upon heating to a certain temperature (typically 50-70℃ in my experiment), ammonia borane molecules decompose into three products: hydrogen, polyiminoborane, and borazine (Figure 1.3) [7].

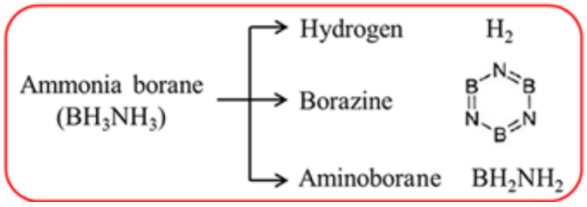

Figure 1.3: Chemical reaction of ammonia borane when it is heated up to a certain temperature

These products diffused into the furnace where they were adsorbed onto the copper foil (This step depends on the binding energy between the borazine molecule and the substrate.). At high temperature, borazine ($B_3H_6N_3$) and aminoborane (BH_2NH_2) would decompose into BN clusters and diffuse on the Cu substrate. Nucleation proceeded at several sites on the Cu surface and the active BN radicals would attach to the growing edges of the triangular domains [8].

Actually, the chemistry of the precursor is quite complicated. For each growth, the growth time is not infinite. In another word, there is a “longest growth time” for each new-loaded precursor. If the growth time exceeds this longest growth time, the

precursor powder may melt and the precursor supply would stop [6]. Besides that, I also found that the higher the precursor temperature is, the shorter the growth time could be.

CHAPTER 2

FACTORS AFFECTING THE AS-GROWN H-BN QUALITY

Nucleation density is a very important parameter to determine the quality of the h-BN film. The lower the nucleation density is, the larger the single crystal domain size we can get. In this part, I investigated three factors that can affect the nucleation density behavior.

2.1 Growth on Elecrtopolished Copper Foil

As we know, the substrate plays a really important role in affecting the growth. It is known that the presence of grain boundary and impurities on rough substrates can reduce the nucleation energy barrier and thus serve as nucleation seeds to facilitate heterogeneous nucleation [9]. So we can say, the rougher the substrate is, the larger the nucleation density is. In such case it is necessary to smooth the substrate to restrain the nucleation density in order that we can get bigger single grain h-BN flakes. Here we introduced the electropolishing method to improve the copper substrate roughness. (Two pieces of Cu foil (125 μm thick, 99.9%, Alfa-Aesar) was used to do the electropolishing. One served as the anode and the other served as the cathode. They were fixed by an alligator clip and merged into the electropolishing solution (167 mL of water, 63 mL of phosphoric acid and 270 mL of ethylene glycol). A constant current power supply was used to provide the voltage in the range of 12-18 V.

The electropolishing usually proceeded for 10min. After electropolishing, the Cu foil was rinsed with deionized water, further blow-dried with nitrogen [10]). The growth was taken on both polished and unpolished copper simultaneously in order to evaluate their difference. Figure 2.1 shows the SEM images of the as-grown h-BN.

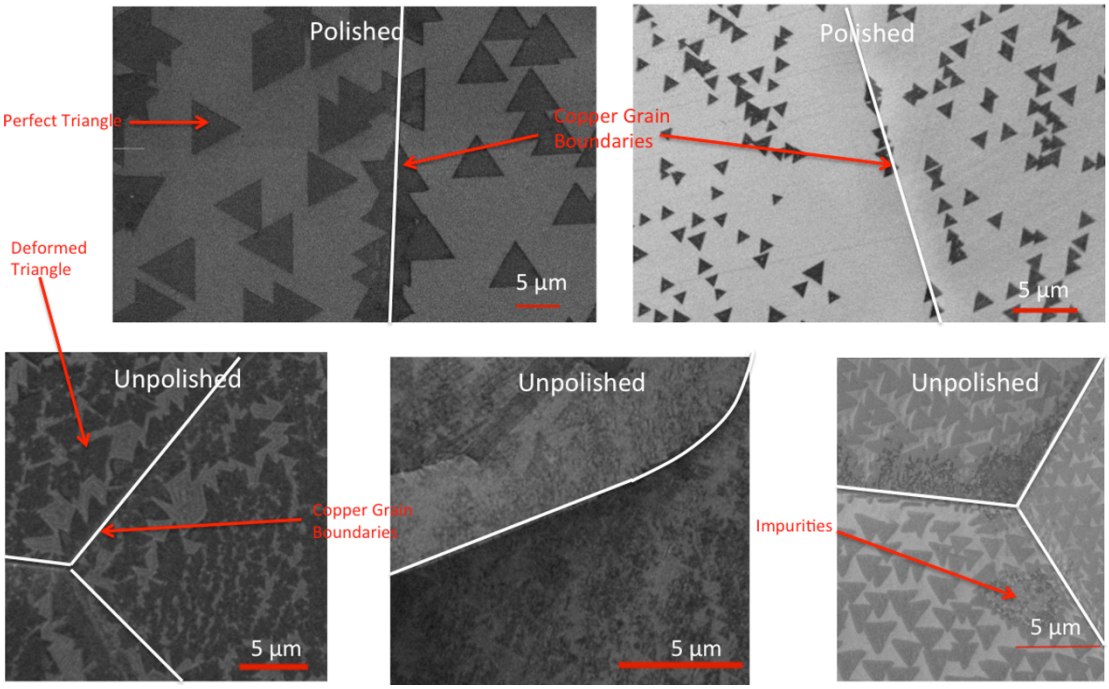

Figure 2.1: SEM images showing the comparison of growth on polished copper substrate and growth on unpolished copper substrate

By comparing the growth results on polished copper foil to that on unpolished copper foil, we can see clearly their contrasting differences in these aspects. 1) Both the exposed copper surface and the BN flakes are cleaner on the polished copper substrate, as compared to those on the unpolished copper; 2) The h-BN domains on the polished copper are perfect triangles while the as-grown triangles on the unpolished copper have negative/positive curved edges; 3) Higher nucleation density on unpolished

copper always makes the triangles grow together. We can hardly see the individual triangles; 4) These triangles on polished copper foil align much better than those on the unpolished copper foil do.

What we are most considering about is the quality of as-grown h-BN film. The nucleation density (ND) to a large extent determines the quality of the materials. By

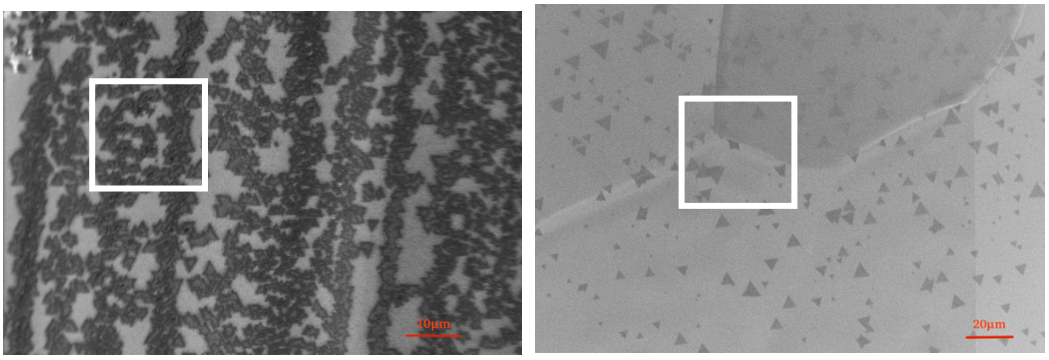

Figure 2.2 Showing how the nucleation density is calculated

calculating the nucleation density we got the ND on polished substrate is about $5 \cdot 10^5 - 8 \cdot 10^5\ mm^{-2}$ and the ND on unpolished substrate is about $3 \cdot 10^3 - 5 \cdot 10^3\ mm^{-2}$. The number of the individual domains was first counted in the marked square and then converted into the nucleation density (Figure 2.2). By comparing we can find that the nucleation density on the unpolished copper foil is ~100 times larger than that on the polished foil. It's a huge improvement. For the following parts, all the growth is taken on the polished copper substrate.

Fig.2.3 shows a series of SEM images demonstrating the growth pattern with different growth time. The growth parameters are listed below.

Growth Temperature	Precursor Temperature	H_2 Flow Rate	Substrate
1020℃	70℃	10 sccm	Polished Copper

Table 1.1: Growth parameters

From this series of images we can find that 1) The grain size of the individual triangles is about 20-30μm; 2) The individual flakes began to coalesce after 40min; 3) After 60min of growth the coalesced film was formed; 4) Rare bilayer structure was formed although the growth time was prolonged after the first layer was coalesced.

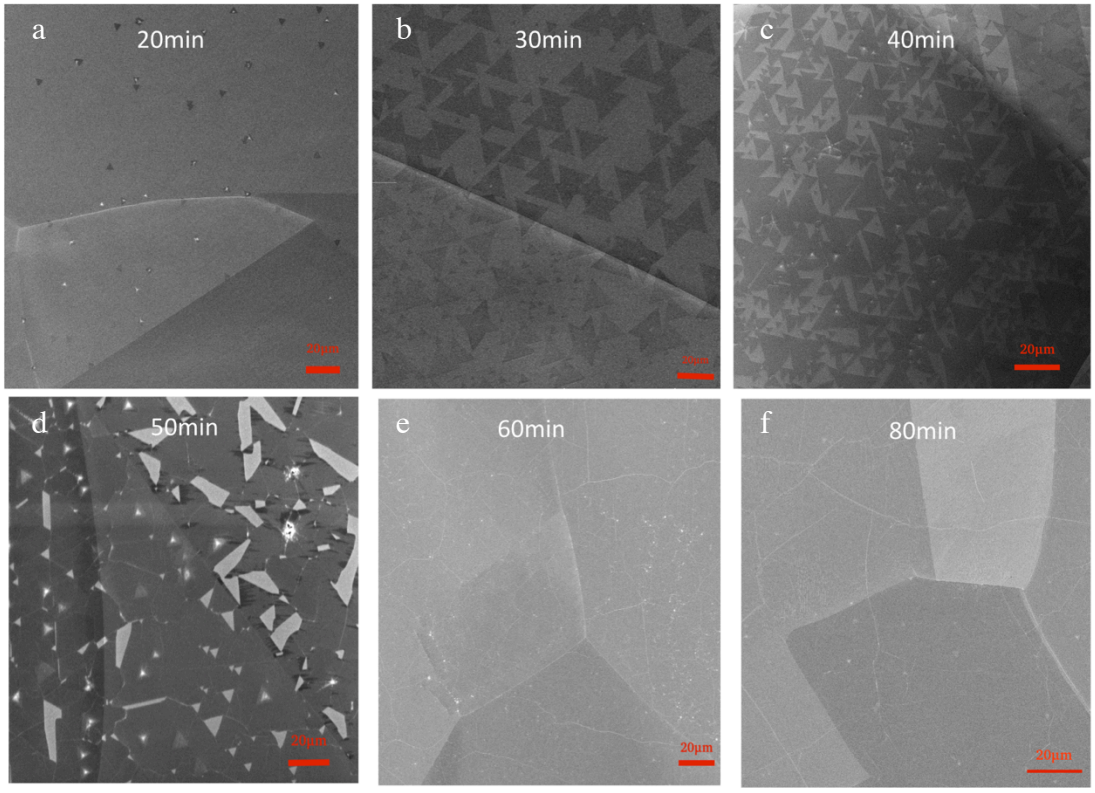

Figure 2.3: SEM images showing the growth results with different growth time: a) 20min b) 30min c) 40min d) 50min e) 60min f) 80min

Fig.2.4 shows the plot of the growth size as a function of growth time at different growth time. The grain size is defined by the side length of each h-BN triangular flake.

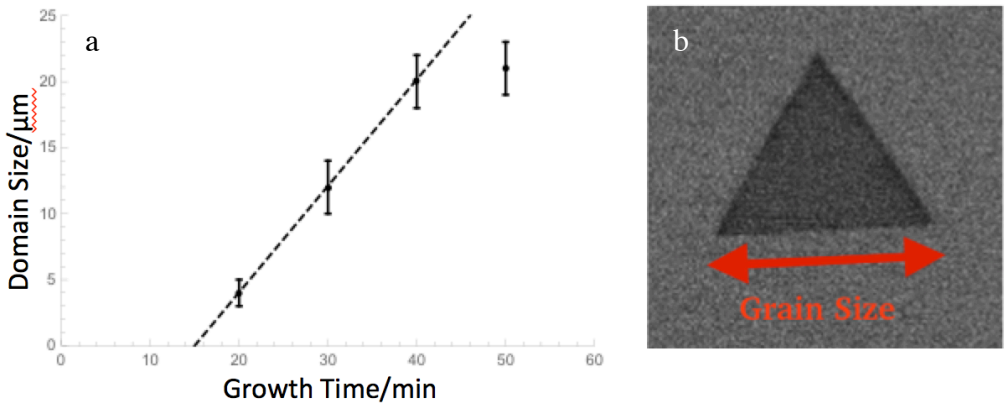

Figure 2.4: a) Plot of grain size as a function of the growth time b) Illustration of how to determine the grain size

From the plot, we can find that before the triangles grew together, the growth rate was constant. The growth did not happen at the very beginning. There was an incubation time. The incubation time can be estimated by the linear fitting. The intersecting point of the linear fitting line and the time axis indicates the incubation time. It is about 15 min with the growth parameters mentioned above,

2.2 Growth with different bubbler temperature

In this section, I investigated the influence of precursor concentration on the resulting growth pattern. The bubbler temperature plays a role in controlling the precursor concentration. In such case, we varied the different bubbler temperature (50C, 60C, 65C, 70C，75C) to see how the growth result is affected.

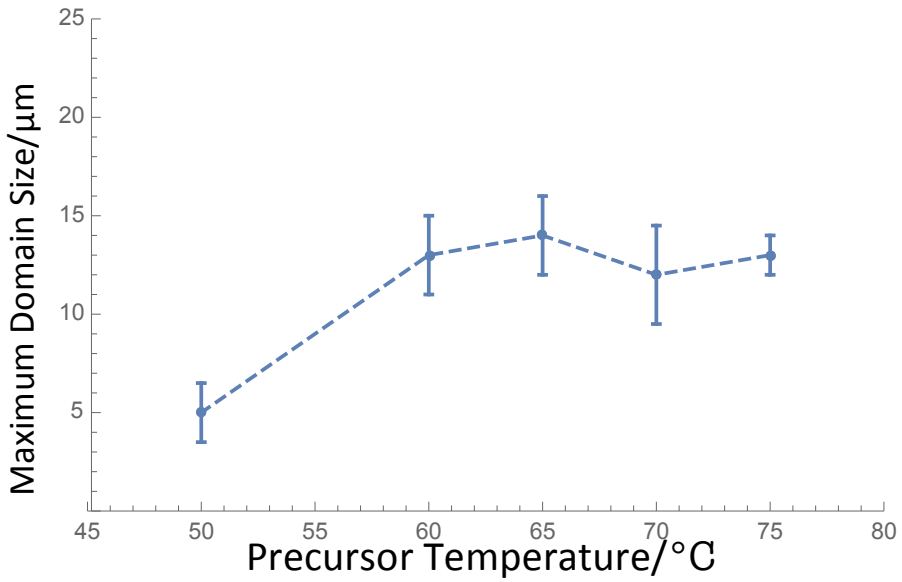

Figure 2.5：plot of domain size as a function of the different bubbler temperature.

Fig.2.5 shows the plot of the domain size as a function of the different bubbler temperature. The as-labeled domain size is the maximum individual domain sizes that the h-BN flakes could reach before they begin to grow together. We found that the domain size was small when the bubbler temperature was below 55 C. As the temperature was above 55C, the domain size did not change too much. My experiments show when the precursor temperature was 50C, coalesced film could not be obtained. At 55C, the ratio between the precursor and hydrogen was low. I ascribe the smaller domain size at 50C to the equilibrium between the hydrogen etching and the h-BN growth. When the temperature was above 55C, the concentration of precursor should increase with the heating belt temperature. However, since the gap between the copper foil and the boat was very small, the vapor pressure of copper was much higher. That made the precursor hardly diffused into that area freely. Higher

concentration of precursor in the free space didn't mean higher concentration in the growth area. Copper vapor pressure played a role in restraining the precursor amount in the growth area. In such case, the precursor concentration saturated when the bubbler temperature is above 55C. This made the domain size/ nucleation density didn't show much variation with the heating belt temperature.

According to the research [6] that how long that a new AB sample would melt, we know we have about 20 hours prior to melting at 75C but only 4 hours at 80C. Since reducing the bubbler temperature would not influence the nucleation performance too much, if we want to process a long time growth, reducing the bubbler temperature may be a way to avoid the melting of precursor.

2.3 Growth with tunable gap size

In this section, I investigated how the gap spacing influences the h-BN growth. I tuned the gap between the copper foil to the quartz boat from 500μm to 0 μm. The gap was formed through the assistance of different thickness wafer. The method is sketched below (Figure 2.6):

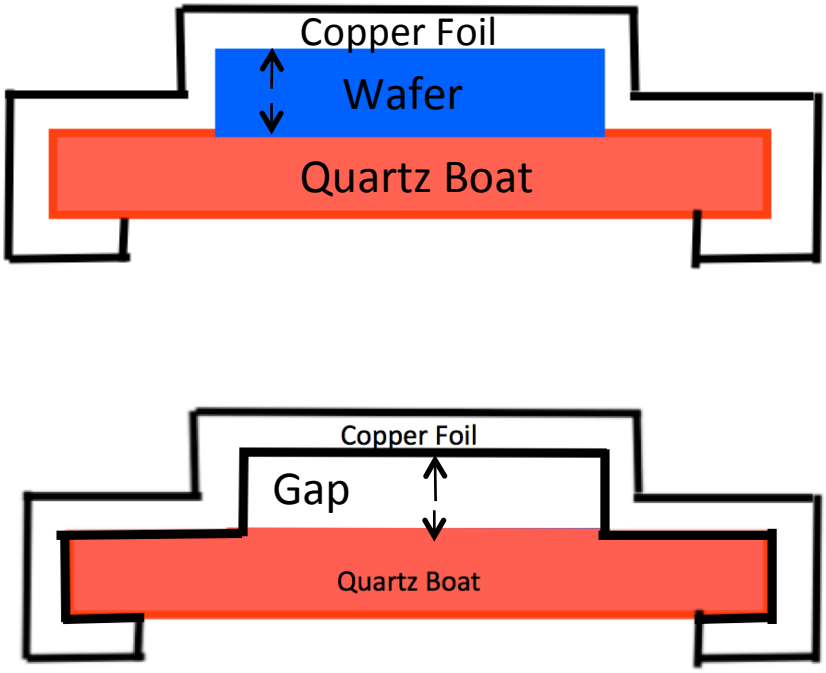

Figure 2.6: Intersecting surface showing how the copper foil wraps on the boat. a) Before removing the wafer and b) After removing the wafer.

First I placed a wafer on the quartz boat and then I wrapped the copper foil on top of it. After squeezing the foil carefully, I removed the wafer and thus the gap was formed. The size of the gap was determined by the thickness of the wafer. The gap size I used was 500μm, 250μm, 125μm and 0μm.

Fig. 2.7 shows the growth results in 15min as the gap spacing was tuned. From the images we can see that for the 0 gap case. There was no growth in 15 min. And the larger gap spacing was, the higher the coverage of h-BN could be. The coverage is the combination effect of the nucleation rate, nucleation density. Considering this, I'd like to know how the gap size affecting these factors.

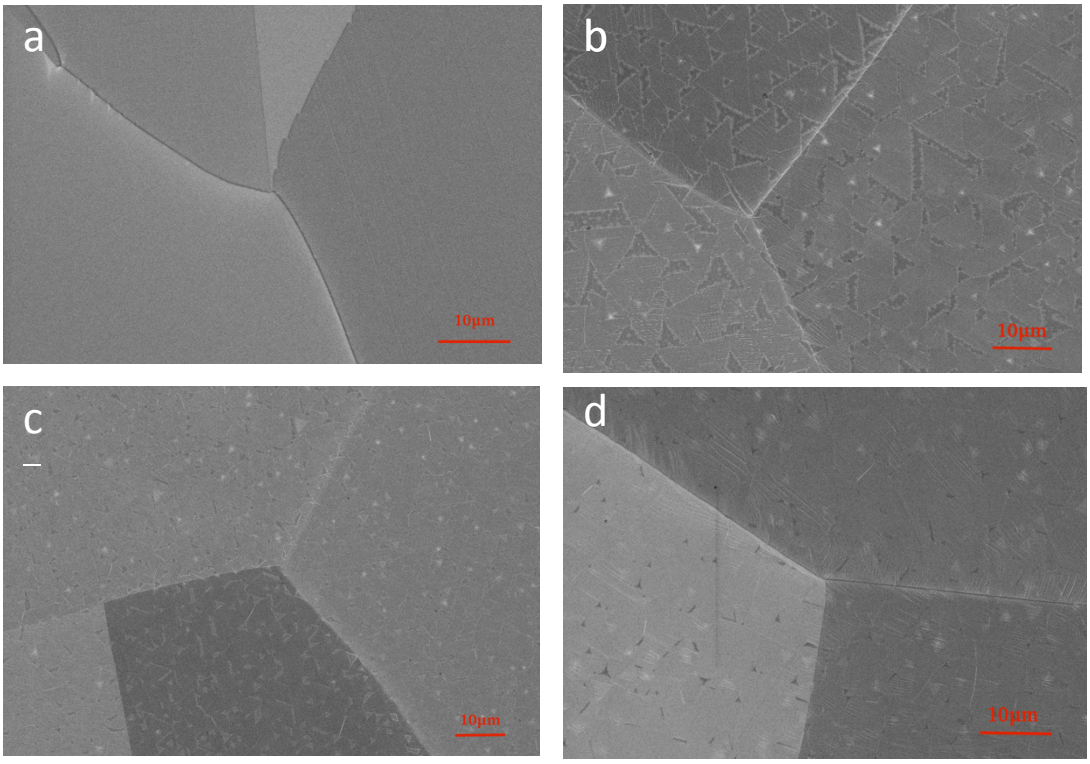

Figure 2.7: Growth results in 15min as the gap spacing is tuned. a) 0 μm; b) 125 μm; c) 250 μm; d) 500 μm

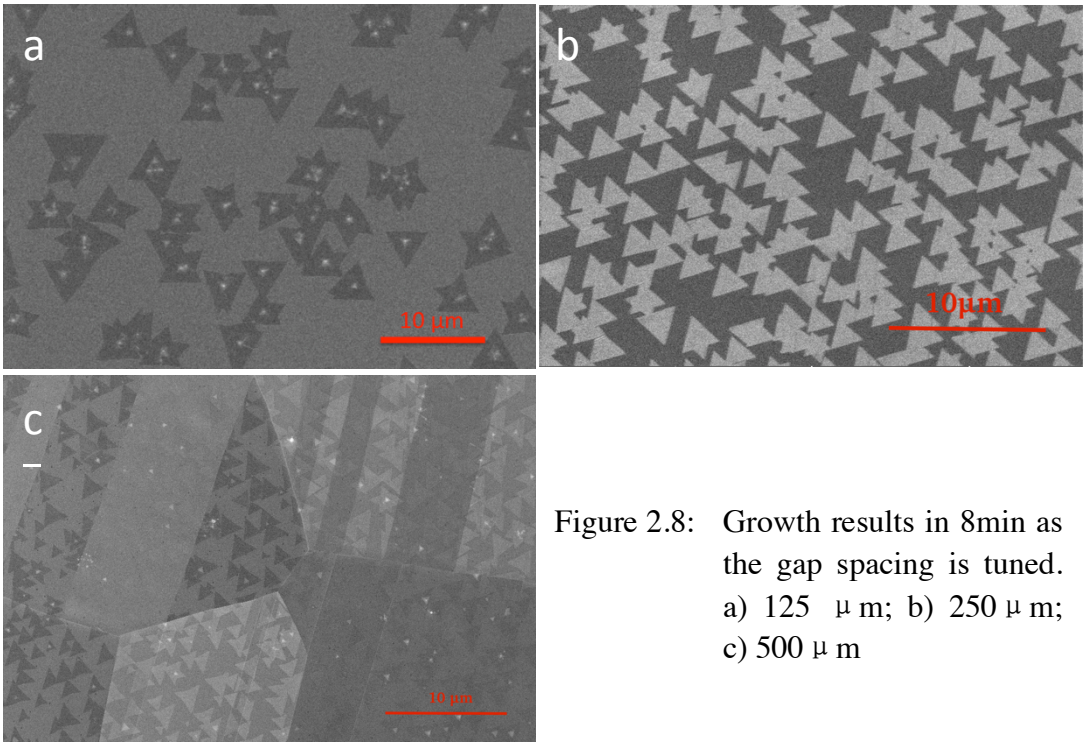

Figure 2.8: Growth results in 8min as the gap spacing is tuned. a) 125 μm; b) 250 μm; c) 500 μm

Since in 15min growth, the h-BN flakes were almost coalesced. Considering this, I reduced the growth time to 8min and figure 2.8 shows the result. It is clearly that the nucleation density increased with the increase of the gap size.

2.3.1 Incubation time

According to what I have discussed above in section 2.1 that the growth rate is almost constant, the incubation time of the nuclei can be estimated by linear fitting of the flake size and the growth time. The time corresponds to 0 size is the incubation time. Fig. 2.9 shows the growth size as a function of growth time.

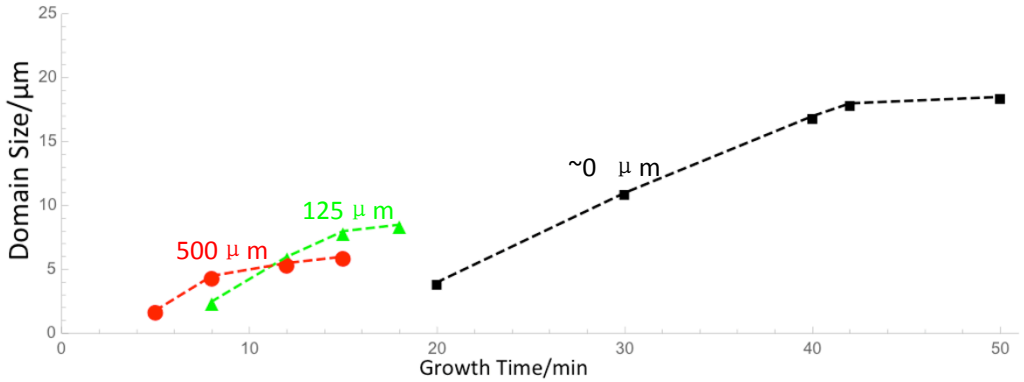

Figure 2.9: Grain size as a function of growth time

By elongating the fitting line and intersecting it with the growth time axis, we can have the incubation time for varied gap spacing: 0μm-15min, 125μm-6min, 250μm-3.5min, and 500μm-3.5min. This result demonstrates the relationship between the gap spacing and the incubation time straightforwardly: the larger the gap is, the faster the nucleation rate would be. However, when the gap size reached 250 μm, the nucleation rate began to saturate.

2.3.2 Nucleation Density

Another phenomenon I observed is that the gap size can affect the h-BN flake size/nucleation density as well. From the SEM images taken from the 8min growth, we can see that the ND would vary with the different gap size.

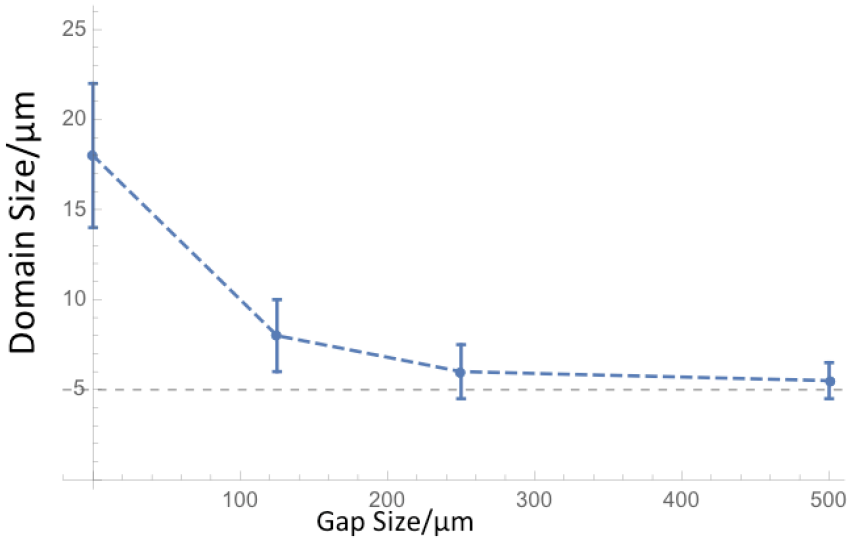

Figure 2.10:Domain Size as a function of gap size

Fig.2.10 shows that the nucleation density clearly increased as the gap spacing increased and saturates as the gap spacing reaches 100 µm. As we know, the larger the gap size was, the easier for the precursor molecules to diffuse into the gap spacing. As the growth area was a confined structure, it may indicate the conversion from Knudsen diffusion to free diffusion. To make it clearly I did some calculation. The mean free path for the precursor is calculated as follows.

$$\lambda = \frac{k_B T}{\sqrt{2}\,\pi\sigma^2 p}$$

Among this calculation I used borazine as the precursor since it is the most reasonable h-BN film building block according to the recent research [11].$k_B$is Boltzmann constant and T is the furnace temperature. σ is the particle hard shell diameter for borazine and p is the chamber pressure. The as-calculated mean free path is 67 μm. Therefore, when the gap size is smaller than 100 μm we can attribute the precursor molecule diffusion to Knudsen diffusion; When the gap size is larger than 100 μm, we can attribute the precursor molecule diffusion to free diffusion. It is consistent with the phenomenon we observed in the tunable gap experiment.

CHAPTER 3

H-BN ETCHING

In this section, etching of h-BN triangles was investigated. In the etching process, precursor was stopped after the growth of h-BN was completed (The growth parameters are same as those listed in Table 1.1). Right after that, a certain ratio of Ar/H2 mixture was flowing for a period of time while keeping the furnace temperature same as the growth temperature. During the post-growth etching, the chamber pressure was fixed at 8 torr. The motivation for studying the etching behavior is to do growth-etching-regrowth experiment to get high quality h-BN.

3.1 Etched Pattern with Different Flow Ratio

In this section we demonstrate the observation of a serious of etched patterns, containing rounded h-BN triangles, perfect h-BN triangles, negative curved h-BN triangles and dendritic shapes. These phenomena tell us that the well-known edge-attached-controlled mode and diffusion-controlled mode that are used to explain various similar materials growth results [12] are also attributed to the shaping of these etched h-BN patterns. This result reveals a post-growth method for engineering the shape of the h-BN individual domain.

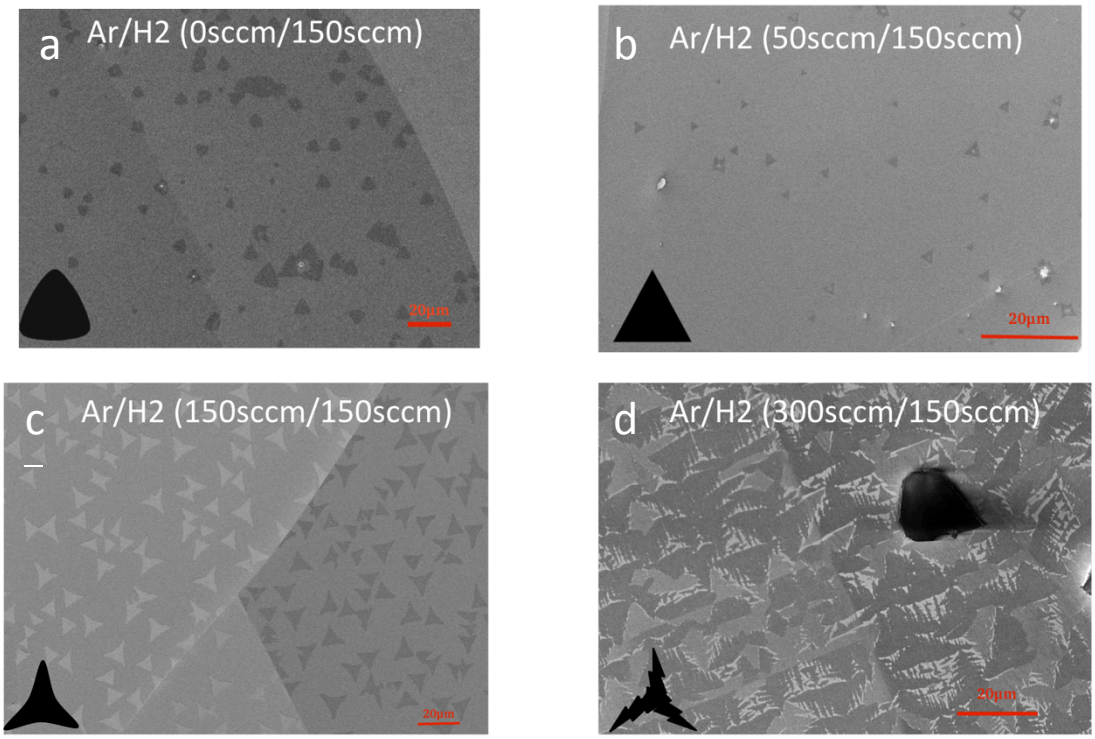

Figure 2.10:Individual etched patterns obtained at various Ar/H2 flow rate ratios

Figure 2.10 shows a series of SEM images of the etching result with varied Ar/H2 flow rate ratios. When the Ar/H2 flow rate ratio was low (20 sccm/ 150sccm) during the etching experiment, rounded triangles were observed after etching. This phenomenon is consistent with the previous published result [13]. As the Ar/H2 flow rate ratio gradually increased to 50 sccm/ 150sccm and further to 50 sccm/ 150sccm, the edge of the triangular etched domain gradually tuned from positive curved to straight and then to negative curved. Further increasing Ar/H2 (300 sccm/ 150sccm) ratio resulted in dendritic shaped etched domains.

From Figure 2.10 we can find that the etched patterns clearly ranged from compact shape to dendritic shape. According to the previously reported etching experiments

for other 2D materials such as graphene [14], we can ascribe the rounded shape to the Attachment-controlled mode while ascribing the dendritic shape to the Diffusion controlled mode. For the attachment-controlled mode, the rate of the etched atoms to diffuse away from the h-BN domains is slow. These atoms have enough time to diffuse along the outside of the domain edges to find the most energetically favorable sites. In such case, the compact etched patter is formed. For the diffusion-controlled mode, the rate of the etched atoms to diffuse away to the etched area is fast. The etched atoms do not have enough time to diffuse along the h-BN flakes. The most energetically favorable removal of etched atoms is impeded thus the dendritic structure is formed.

Back to our experiment, total chamber pressure was fixed. When the flow rate ratio was low (Ar/H2: 0sccm/ 150sccm), the concentration of hydrogen was high. Higher hydrogen concentration resulted in more H radicals absorbed on Cu. The H radicals could serve as barriers to impede the diffusion of the etched B and N atoms thus leading to low diffusion rate. This corresponds to attachment-controlled mode. When the flow rate ratio was high (Ar/H2: 300sccm/ 150sccm), the concentration of hydrogen was low. Lower hydrogen concentration resulted in less H radicals absorbed on Cu. The H less radicals led to high diffusion rate. This corresponds to diffusion-controlled mode.

3.2 Etched Holes

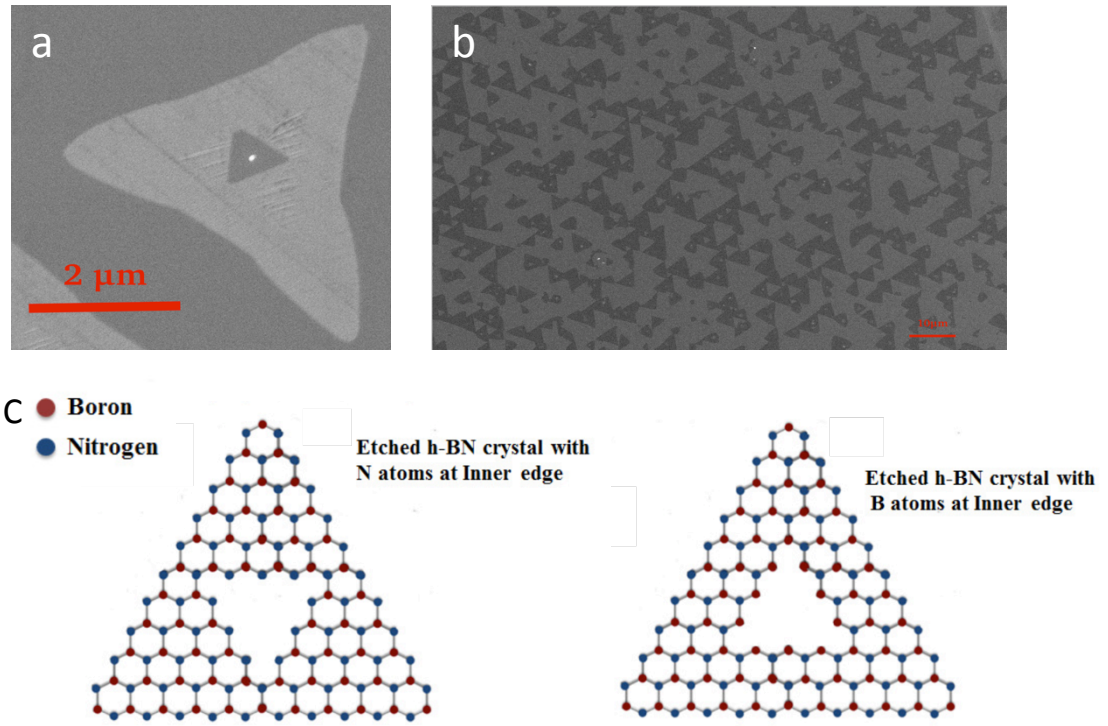

Figure 2.11:a) and b) etched h-BN triangular domains with holes in the center. c) Atomic schematic illustration of etched holes

During the etching experiments I also observed some etched holes created in the center of the h-BN individual triangles and the shapes of the holes were triangles as well. What I further observed was that the orientation of the triangular holes was in the opposite direction to the orientation of the outside h-BN triangular domain. Fig. 2.11c illustrates the atomic schematic representation and we can find that if the orientation is same then the hole is nitrogen-terminated while if the orientation is opposite then the hole is boron-terminated. It is reported [15] that for h-BN N-terminated edges is energetically favorable than these of B-termination. Our result is consistent with the theoretical calculation.

CHAPTER 4

CHARACTERIZATION

4.1 Characterization Tools and Techniques

Reflection Raman Microscopy: Samples were transferred on to SiO_2 substrate and Raman characterization was accomplished via a Renishaw InVia Confocal Raman microscope. The excitation frequency of the laser was at a wavelength of 488 nm.

X-ray photoelectron spectroscopy (XPS): Samples were transferred on to a SiO_2 substrate and was pre-heated in the load-lock before moving into the main chamber for characterization.

LEEM I-V Curve: It was a homemade system and the introduction of the system is listed in ref. [18].

Device fabrication: The h-BN was transferred using a wet transfer approach and then was spun PMMA 4% at 3000rpm for 60s. The stack was then left to float in Cu etchant CE-100 from Transene for 12hrs. The floating PMMA/hBN layer was then transferred to DI water and left to float for another 12hrs. after this the PMM/hBN was scooped up in the target substrate and left to dry for 12hrs. Finally the PMMA/hBN on the target substrate was left in a solvent solution (Microposit remover

1165 from Shipley) for 12hrs. to remove the PMMA layer. The target substrate used in this study was SiO2(280nm) on p-type doped Si.

4.2 XPS

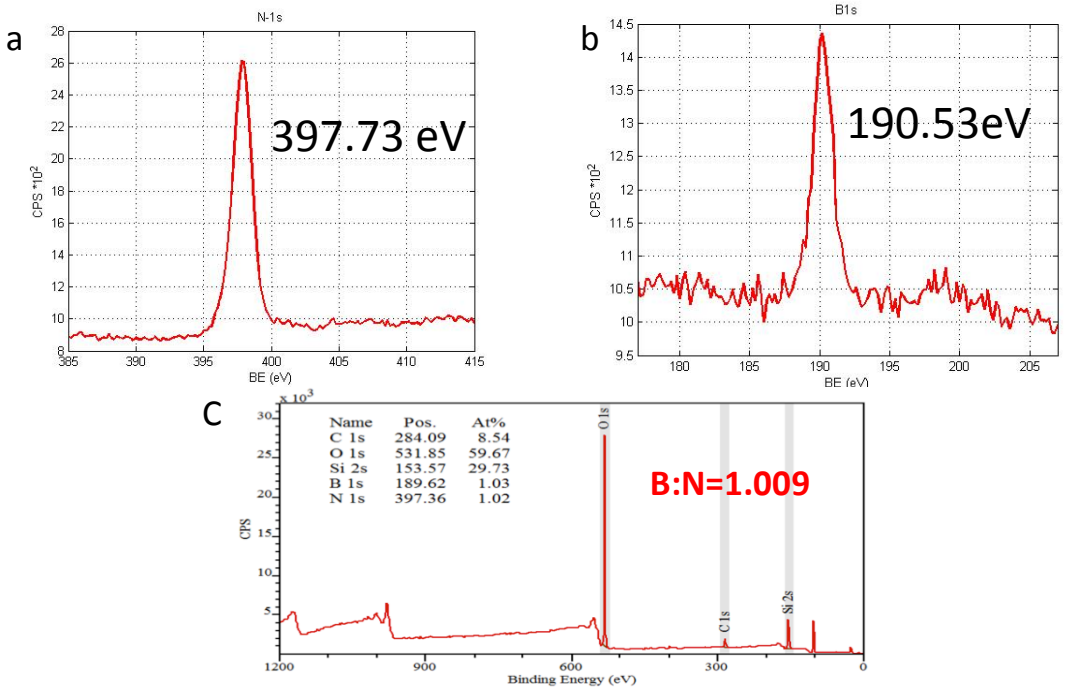

Figure 4.1: a) N 1s peak b) B 1 s peak c) XPS Survey scan

XPS was used to check the existence of B and N and to determine the B/N element ratio. The B/N ratio from the XPS survey scan was found to be 1.009. The closer of the ratio is to 1, the higher the quality of the as-grown h-BN could be. 1.009 indicates very high quality. The binding energies of N 1s and B 1s from the B 1s and the N 1s spectra are 397.73 and 190.53 eV which indicate that the B and N atoms are in the B-N bonding. That means the presence of hexagonal boron nitride in my growth [16].

4.3 Raman

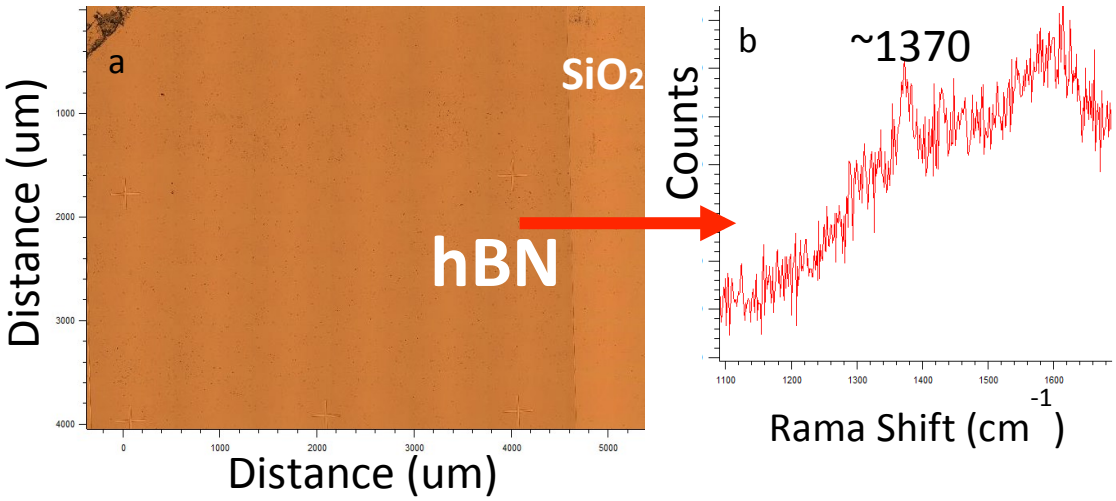

Figure 4.2: a) Optic microscope image b) Raman Microscopy with a peak at 1379 cm^{-1}

Raman was also used to check the presence of hexagonal boron nitride in my growth. Figure 4.2s is the optic microscope image showing where we did the measurement and we can see clearly the contrast between the bare SiO2 substrate and the transferred h-BN film. From figure 4.2b we observed a Raman peak at 1370 cm^{-1}. It is consistent with the h-BN film Raman peak corresponding to the E2g vibration mode of h-BN [17].

LEEM I-V Curve

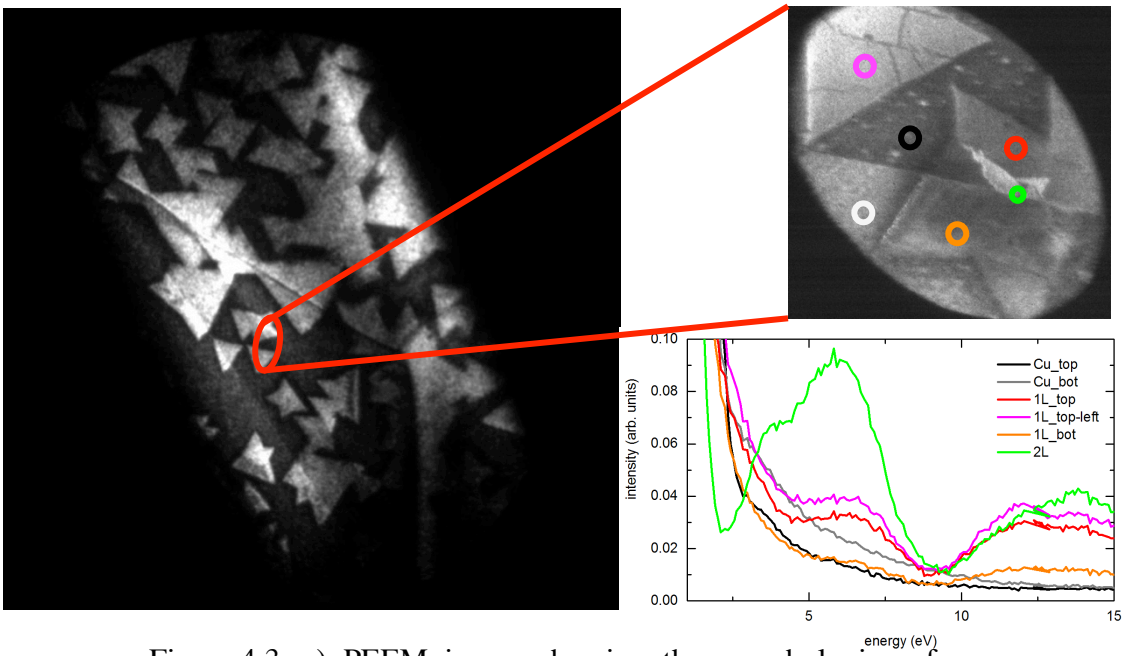

Figure 4.3: a) PEEM image showing the morphologies of the as-grown h-BN b) amplified PEEM image showing where we did the measurements c) IV-curves reflecting electron intensity as a function of landing energy

LEEM IV-curves was used to determine the layer number of our as-grown h-BN. monolayer, bilayer h-BN and bare Cu surface, respectively (Fig. 4.3c). For layered materials, there is an unoccupied state in each gap between the adjacent layers. The number of the unoccupied states is corresponding to the number of minima. This is the mechanism how to measure the layer number. From Fig. 4.3a,b. we can identify clearly the layer number by the significant contrast. It is consistent with what we got from the LEEM I-V Curve.

4.5 Diffusive Space-charge Current

The fabrication procedure consisted of only two layers, the first being the alignment markers and the second being the contact definition. The contacts were Ni electrode for this study since it has been found to serve as an ohmic contact in prior studies [19-20]. Figure 4.4 shows the device construction. The width of the h-BN channel is about 1 μm.

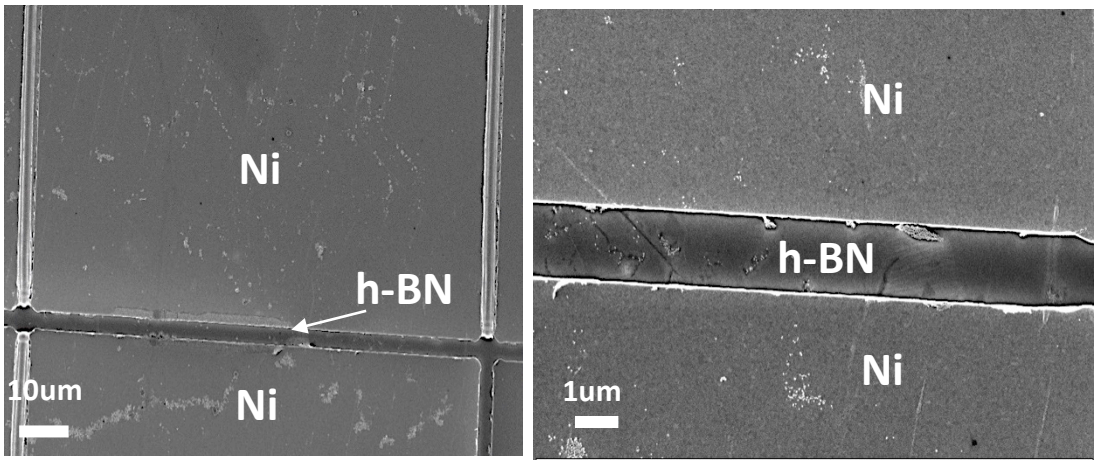

Figure 4.4: SEM images showing the device construction

In Figure 4.5 we can see current-voltage (I-V) characteristics of a typical devices at a channel width of 1um. Figure 4.6 shows current as a function of voltage squared and reveals the nature of the transport in our h-BN which we believe to be space charge limited [19]. The bias voltage and the current has the relationship: $I \alpha V^{\lambda}$ where $1.75<\lambda<2.5$. The value of λ is mainly modified by charge traps and defects in the hBN film. For our devices we find that λ=2 consistent with the Mott-Gurney theory of space charge conduction. The mobility was calculated using equation (1) where ζ=0.7 was used and $\epsilon_o = 8.85e-12\ (F/m)$, $\epsilon_r = 3$ was taken as the average constant of

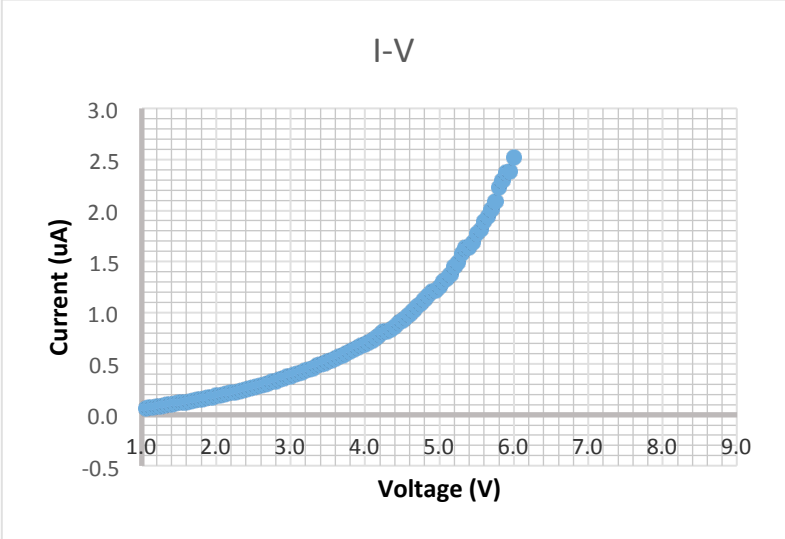

Figure 4.5: Current-voltage (I-V) characteristics of a typical device at a channel length of 1um

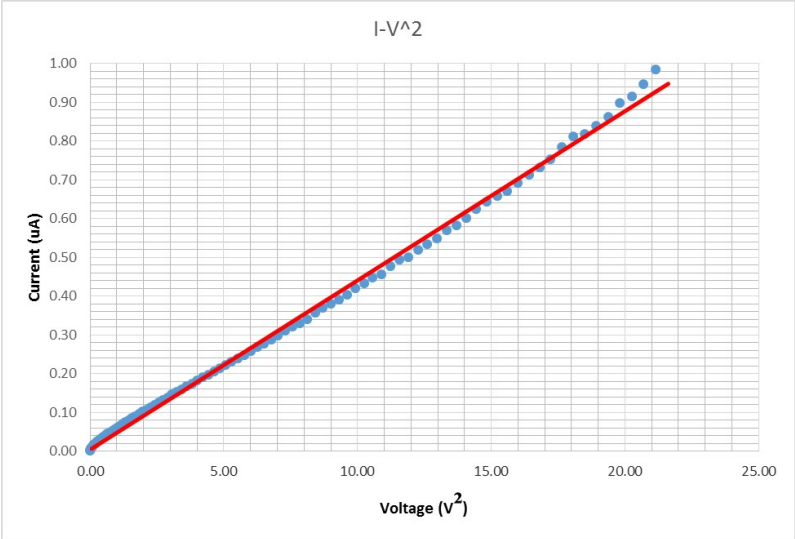

Figure 4.6: The plot of the current as a function of voltage squared shows the current's quadratic dependence on voltage.

the oxide ($\epsilon_r = 3.9$), vacuum ($\epsilon_r = 1.0$) and hBN ($\epsilon_r = 19 - 20\ [ref]$). We estimate a value of μ~0.6457 $^{cm^2}/_{V.s}$ which is at least an order of magnitude than previously reported [3].

$I = \zeta \epsilon_o \epsilon_r \mu \frac{W}{L^2} V$ ..... Eqtn. (1)

CHAPTER 6

CONCLUSION

My research focuses on the controllable growth of h-BN on copper substrates using the low-pressure chemical vapor deposition (LPCVD) method. My main target is to get larger single grain size h-BN film. In order to optimize the growth condition, I investigated how the precursor, geometric environment, substrate engineering and gas mixture affect the quality of the as-grown h-BN. I found that the nucleation density of the as-grown h-BN is a function of the substrate roughness and geometric growth environment. Large grain size and high quality h-BN was obtained. The size is ranging from 20 μm to 30 μm. The evolution of the etched pattern shapes are observed and well explained by the etching mode. The etching experiment reveals a post-growth method for engineering the shape of the h-BN individual domain. Raman, SEM, XPS, and LEEM I-V Curve was performed on the samples for characterization. In the last part, I showed the electric properties of the device made by the as-grown h-BN. Space charge limited current of the device made by the as-grown h-BN was observed.

REFERENCES

[1] Watanabe, Kenji, Takashi Taniguchi, and Hisao Kanda. "Direct-bandgap properties and evidence for ultraviolet lasing of hexagonal boron nitride single crystal." *Nature materials* 3.6 (2004): 404-409.

[2] Watanabe, Kenji, et al. "Far-ultraviolet plane-emission handheld device based on hexagonal boron nitride." Nature photonics 3.10 (2009): 591-594.

[3] Dean, Cory R., et al. "Boron nitride substrates for high-quality graphene electronics." Nature nanotechnology 5.10 (2010): 722-726.

[4] Maissel, Leon I., and Reinhard Glang. "Handbook of thin film technology." (1995).

[5] Ohring, Milton. Materials science of thin films. Academic press, 2001.

[6] Frueh, Samuel, et al. "Pyrolytic decomposition of ammonia borane to boron nitride." Inorganic chemistry 50.3 (2010): 783-792.

[7] Baitalow, F., et al. "Thermal decomposition of B–N–H compounds investigated by using combined thermoanalytical methods." Thermochimica Acta 391.1 (2002): 159-168.

[8] Lu, Guangyuan, et al. "Synthesis of large single-crystal hexagonal boron nitride grains on Cu–Ni alloy." Nature communications 6 (2015).

[9] Tay, Roland Yingjie, et al. "Growth of large single-crystalline two-dimensional boron nitride hexagons on electropolished copper." Nano letters 14.2 (2014): 839-846.

[11] Wang, Lifeng, et al. "Monolayer Hexagonal Boron Nitride Films with Large Domain Size and Clean Interface for Enhancing the Mobility of Graphene‐Based Field‐Effect Transistors." Advanced Materials 26.10 (2014): 1559-1564.

[12] Satio, Y. Statistical Physics of Crystal Growth; World Scientific: Singapore, 1996.

[13] Xie, Liming, Liying Jiao, and Hongjie Dai. "Selective etching of graphene edges by hydrogen plasma." Journal of the American Chemical Society 132.42 (2010): 14751-14753.

[14] Geng, Dechao, et al. "Fractal etching of graphene." Journal of the American Chemical Society 135.17 (2013): 6431-6434.

[15] Liu, Yuanyue, Somnath Bhowmick, and Boris I. Yakobson. "BN white graphene with “colorful” edges: The energies and morphology." Nano letters 11.8 (2011): 3113-3116.

[16] Kim, Ki Kang, et al. "Synthesis of monolayer hexagonal boron nitride on Cu foil using chemical vapor deposition." Nano letters 12.1 (2011): 161-166.

[17] Shi, Yumeng, et al. "Synthesis of few-layer hexagonal boron nitride thin film by chemical vapor deposition." Nano letters 10.10 (2010): 4134-4139.

[18] Jobst, Johannes, et al. "Nanoscale measurements of unoccupied band dispersion in few-layer graphene." Nature communications 6 (2015).

[19] F. Mahvash, E. Paradis, D. Drouin, T. Szkopek and M. Siaj, "Space-Charge Limited Transport in Large-Area Monolayer Hexagonal Boron Nitride," Nano Letters, vol. 15, pp. 2263-2268, 2015.

[20] H. Zeng, C. Zhi, Z. Zhang, X. Wei, W. Guo, Y. Bando and D. Goldberg, ""White Graphenes": Boron Nitride Nanoribbons via Boron Nitride Nanotube Unwrapping," Nano Letters, vol. 10, pp. 5049-5056, 2010.